Measurement of ^{232}Th(p, x)^{225}Ac reaction cross-section at CSNS APEP facility up to 80 MeV*

Bing Jiang,[1,2] Binbin Tian,[1,2] Hantao Jing,[1,2,†] Qifan Dong,[1,2,3] and Lu Guo[3]

[1]*Spallation Neutron Source Science Center, Dongguan 523803, China*
[2]*Institute of High Energy Physics, Chinese Academy of Sciences (CAS), Beijing 100049, China*
[3]*University of Chinese Academy of Sciences, Beijing 100049, China*

The radioisotope actinium-225 (^{225}Ac) has been successfully used for targeted alpha therapy in preclinical and clinical applications because of its excellent nuclear characteristics. Medium- and high-energy proton-spallation reactions on thorium are the most important methods for producing ^{225}Ac. This study examines the possibility of producing ^{225}Ac by irradiating thorium oxide with medium-energy protons. Thorium-oxide sheets were irradiated with 40-, 50-, 60-, 70-, and 80-MeV protons on the Associated Proton-beam Experiment Platform (APEP) of the China Spallation Neutron Source (CSNS). The cross sections for the formation of ^{225}Ac were measured using the activation method and offline gamma-ray spectrometric technique. The experimental results were compared with the existing data from EXFOR as well as the theoretical data from the TALYS-based evaluated nuclear-data library. Based on the experimental cross section and theoretical calculations, the production yield of ^{225}Ac in the irradiated thorium targets was examined. The results showed that APEP can produce sufficient quantities of ^{225}Ac for purification and clinical therapy. This work is the first measurement of proton-induced nuclear-reaction cross sections at the CSNS APEP.

Keywords: ^{232}Th target; Proton irradiation;^{225}Ac producing cross section; CSNS APEP

I. INTRODUCTION

Targeted alpha therapy (TAT) is a promising and effective future tumor therapy[1]. In this therapeutic application, selected alpha-emitting radioisotopes are delivered to cancerous tissues within the body. They can kill cancer cells that are resistant to treatment with β^- or γ irradiation, as well as radiopharmaceuticals. The alpha-emitting radioisotope actinium-225 (^{225}Ac) has been identified as one of the most promising candidates for TAT because of its suitable half-life ($T_{1/2}$=9.9 d, 100% α decay) and short range in tissues[2]. The long half-life of ^{225}Ac enables a slow decay during its production and delivery. The alpha particles released by ^{225}Ac have a high linear energy transfer, depositing energy at an average rate of approximately 100 keV/μm and traversing a mere 50–90 μm within biological tissue. This combination of high-energy deposition and a limited range is ideally suited for obliterating tumor cells while sparing adjacent healthy tissues, thereby enhancing the therapeutic index. However, the application of ^{225}Ac radiopharmaceuticals still faces significant challenges, including a limited isotope supply and difficulties in chemical separation.

The existing ^{225}Ac available for clinical studies was derived from the decay of long-lived ^{229}Th ($T_{1/2}$ = 7880 y), which decays from ^{233}U ($T_{1/2}$ = 1.592×10^5 y)[3, 4]. Unfortunately, the supply of ^{225}Ac is low because of the limited stock of ^{233}U. The approval of multiple treatments using ^{225}Ac requires alternative production methodologies. A promising route for producing ^{225}Ac is the irradiation of natural ^{232}Th targets with medium- and high-energy protons, followed by product separation[2, 5]. Based on theoretical calculations, ^{225}Ac is produced by several pathways during proton irradiation of ^{232}Th[6]. The major reaction channels for the production of ^{225}Ac via a proton reaction with a ^{232}Th nucleus are shown in Fig. 1. The measurement of the production cross section is crucial, as these data provide essential information for optimizing the production of ^{225}Ac from a Th target and for refining the chemical procedures to isolate ^{225}Ac from the irradiated Th.

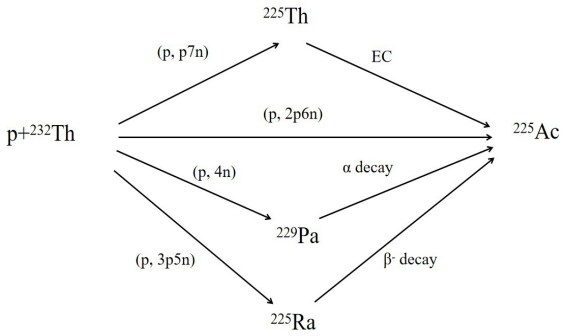

Fig. 1. Major reaction channels for the production of ^{225}Ac from a proton reaction with a ^{232}Th nucleus. The cumulative production cross sections of ^{225}Ac are studied in this work.

In recent years, several measurements of the ^{232}Th (p, x) ^{225}Ac reaction cross section have been performed at different particle-accelerator centers worldwide. All measurements were performed using the offline gamma-ray spectrometric technique. At the iThemba Laboratory for Accelerator-Based Sciences of South Africa, the excitation functions of selected radionuclides in p + ^{232}Th were measured using the well-known stacked-foil technique from the thresholds up to 66 MeV[7]. The effective cross sections for the production of ^{225}Ac at proton energies between 78 and 192 MeV were measured by three laboratories: Brookhaven National Laboratory,

* Supported by the National Natural Science Foundation of China (No.12075135) and the National Natural Science Foundation of China (No.12375127)
† Corresponding author.E-mail:jinght@ihep.ac.cn,Tel:0769-88931990

Los Alamos National Laboratory, and Oak Ridge National Laboratory[8]. At the Los Alamos Neutron Science Center (LANSCE) accelerator facility, the cross sections for the formation of ^{225}Ac and ^{225}Ra via the proton bombardment of natural Th targets were measured at a nominal proton energy of 800 MeV[9]. At the Weapons Neutron Research Facility and LANSCE Isotope Production Facility, two groups of Th-irradiation experiments were conducted to study the production cross sections of ^{225}Ac with proton energies ranging from 56 to 194 MeV[10]. At the Institute for Nuclear Research, Russian Academy of Sciences, Th foils were irradiated with 90-, 110-, and 135-MeV protons to investigate the cumulative production cross sections for ^{225}Ac[6]. Metallic Th foils were used as targets in the cross-sectional measurements of ^{225}Ac at proton energies of 21–141 MeV at the Research Institute of Atomic Reactors [11]. Additionally, irradiation experiments using 100-MeV protons bombarding thorium oxide have also been conducted at the 100-MeV cyclotron at the China Institute of Atomic Energy [12]. Although most of these measurements were carried out with high precision, discrepancies in the ^{232}Th(p, x)^{225}Ac reaction cross section still exist and cannot be ignored. Data from different institutions differ significantly at some energy points in the low-energy region; therefore, further experimental measurements are required to clarify these differences.

The Associated Proton-beam Experiment Platform (APEP)[13] is a new medium-energy proton-irradiation facility at the China Spallation Neutron Source (CSNS)[14–16], which was constructed to carry out irradiation experiments and produce medical radioisotopes. With a suitable proton energy, high proton flux, and the ability to provide a stable proton beam for APEP, ^{225}Ac has become the main radioisotope for research on the production of medical isotopes at the CSNS[17]. By the end of 2025, the yield of ^{225}Ac at the CSNS is anticipated to reach the millicurie level per week because of the APEP power upgrade . This motivated a new experimental measurement of the ^{232}Th(p, x)^{225}Ac reaction cross section to achieve high accuracy. The production and decay schemes for ^{225}Ac in the irradiated ^{232}Th target are shown in Fig. 2. ^{225}Ac is generated via the proton-induced spallation of ^{232}Th, followed by the emission of three alpha particles that ultimately decay to ^{213}Bi, which is another significant medical alpha-emitting radioisotope. In the present work, the production cross section of ^{225}Ac at proton energies from 40 to 80 MeV is determined using the activation method and an offline gamma-ray spectrometric technique. The experimental results presented in this study are cumulative cross sections, which include the effects of all reaction channels shown in Fig. 1. No previous work on the measurement of proton-induced nuclear-reaction cross sections has been performed at this facility. Measuring cross-sectional data at the APEP can, in turn, help with evaluating the feasibility of producing the ^{225}Ac isotope for medical applications in this facility.

The remainder of this paper is organized as follows. Section II provides a description of the experimental details. The cross-section data analysis and correction procedure are described in Section III. In Section IV, experimental cross-section results are presented and discussed. The conclusions are presented in Section V.

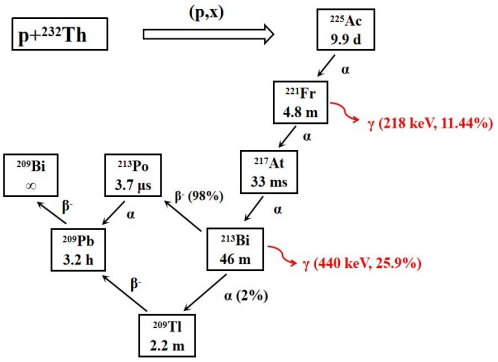

Fig. 2. Production scheme of ^{225}Ac in the irradiated ^{232}Th target. Gamma rays emitted from the daughter isotopes are used to quantify ^{225}Ac.

II. EXPERIMENTAL DETAILS

A. Associated Proton-beam Experiment Platform (APEP)

The CSNS consists of an H- linear accelerator (LINAC), a proton rapid cycling synchrotron, a target station, and multiple experimental spectrometers[18–20]. A proton beamline with medium energy, APEP, is extracted from the end of the LINAC, which is suitable for research on the application of proton irradiation, especially for medical-radioisotope production. Irradiation experiments on Th targets were performed at APEP by utilizing naturally stripped protons extracted from the H^- LINAC at CSNS. The H^--ion beams interact with the residual gas in the vacuum tube, among which a small portion of the H^- ions are stripped into protons and transported to the end of the LINAC. Subsequently, accelerated protons with energies of up to 80 MeV interact with the target nucleus and generate medical radioisotopes of interest. The physical design of the APEP beamline is described in [13].

A schematic of the APEP beamline is presented in Fig. 3 with an actual length of approximately 14.5 m. Two experimental irradiation points, namely, the vacuum test point and air test point (ATP), are located on the beamline at flight-path lengths of approximately 9.3 and 10 m from the extraction position, respectively. Th-irradiation experiments were performed at ATP, which takes advantage of the high proton-energy resolution and low background. A wedge degrader that allows a continuous change in thickness was used to adjust the proton energy within the range of 10—80 MeV. To satisfy various experimental requirements, a three-step cascading collimation system consisting of graphite collimators was employed to control the spot sizes, resulting in spot sizes ranging from 10 mm×10 mm to 50 mm×50 mm at the irra-

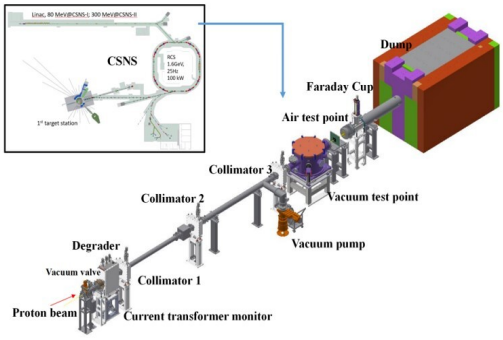

Fig. 3. Schematic of the APEP.

diation points. The main APEP parameters are listed in Table 1, corresponding to an operating power of 100 kW for the CSNS.

Table 1. Main parameters of APEP.

Parameters	Units	Value
Energy (Maximum)	MeV	80
Average current	μA	0.1
Beam pulse length	μs	400
Repetition rate	Hz	25
Proton intensity	p/s	6.24×10^{11}
Beam spot size	mm	10×10-50×50

B. Gamma spectroscopy

Radioactivity measurements were conducted using a well-shielded nitrogen-cooled high-purity germanium (HPGe) detector (GMX 50P4-83, Ortec, USA), which is suitable for high-performance gamma-energy spectral measurements from 3 keV to 10 MeV. PC-based GammaVision-GMX50P4-83 (-3500 V) software was coupled to the HPGe detector. The measured resolution of this detector for the characteristic peak was less than 2.3 keV at 1 MeV and less than 800 eV at 5.9 keV[21]. The energy was calibrated using standard γ sources traceable to the National Institute of Standards and Technology (NIST), including ^{152}Eu, ^{241}Am, ^{60}Co, ^{137}Cs, and ^{40}K. As shown in Fig. 4(a), a sample holder with a thickness of 10 cm was used to reduce the dead time caused by the irradiated samples. The total detector efficiency considering the geometric efficiency is shown in Fig. 4(b).

The γ-ray energies and corresponding branching ratios used in this study were acquired from the National Nuclear Data Center[22]. Several days after the end of bombardment (EOB), the irradiated samples were used repeatedly for gamma-ray spectroscopy. The cooling times were varied for the different irradiated targets to reduce the detector dead time to less than 10%, and the corresponding measurement times were sufficient to ensure adequate statistics. Examples of the spectra collected in this study are presented in the figures. Fig. 5 shows the gamma-ray spectra of the Th target within 5.03 h of irradiation by 80 MeV protons and after 27.76 days of cooling after the EOB. The gamma rays emitted from daughter isotopes ^{221}Fr and ^{213}Bi were used to quantify the amount of ^{225}Ac. The production cross sections of ^{225}Ac were calculated after correcting the resulting activities back to the EOB. The data-analysis method and relevant discussion are described in Section III.

C. Experiment process

Five groups of irradiation experiments were conducted at various time points. As listed in Table 2, the parameters, including the incident proton energy, proton spot size, and irradiation time, were adjusted to satisfy the special requirements of each experiment. The irradiation samples for each experiment consisted of a high-purity (99.9%) ThO_2 sheet and Cu (99.99%) foil, as illustrated in Fig. 6. ThO_2 samples were prepared by high-temperature sintering of the thorium oxide powder. Cu foils were used to monitor the proton-beam flux [21]. During irradiation, the position of the sample holder was remotely adjusted to align the center of the beam with the geometric center of the target.

Table 2. Irradiation parameters.

Energy (MeV)	Mass (g)	Thickness (g/cm^2)	Area (cm^2)	Monitor	Irradiation time (h)	Spot size (mm)
80	1.93	1.98 (0.20 cm)	0.97	Cu	5.0	20×20
70	0.94	1.86 (0.19 cm)	0.51	Cu	40.0	50×50
60	1.37	2.01 (0.20 cm)	0.68	Cu	63.1	50×50
50	2.04	2.05 (0.21 cm)	0.99	Cu	61.5	50×50
40	1.83	1.81 (0.17 cm)	1.01	Cu	45.8	50×50

Before the irradiation experiments, a Monte Carlo simulation was performed using FLUKA[23] to determine the experimental scheme. Using the FLUKA code, we constructed a geometric model for the proton irradiation of the Th target and estimated the activity of ^{225}Ac and the dose rate around the target. In the simulation, the activity of ^{225}Ac reached hundreds of becquerels by the EOB. Considering the dead time of the HPGe detector, the dose rate 10 cm from the target was less than 1 μSv/h. Ultimately, the irradiation time listed in Table 2 was determined based on the simulated activity and corresponding dose rate.

III. DATA ANALYSIS

A. Proton-energy resolution

As described in Section II A, proton energy is moderated by a graphite-based degrader. The proton undergoes Coulomb

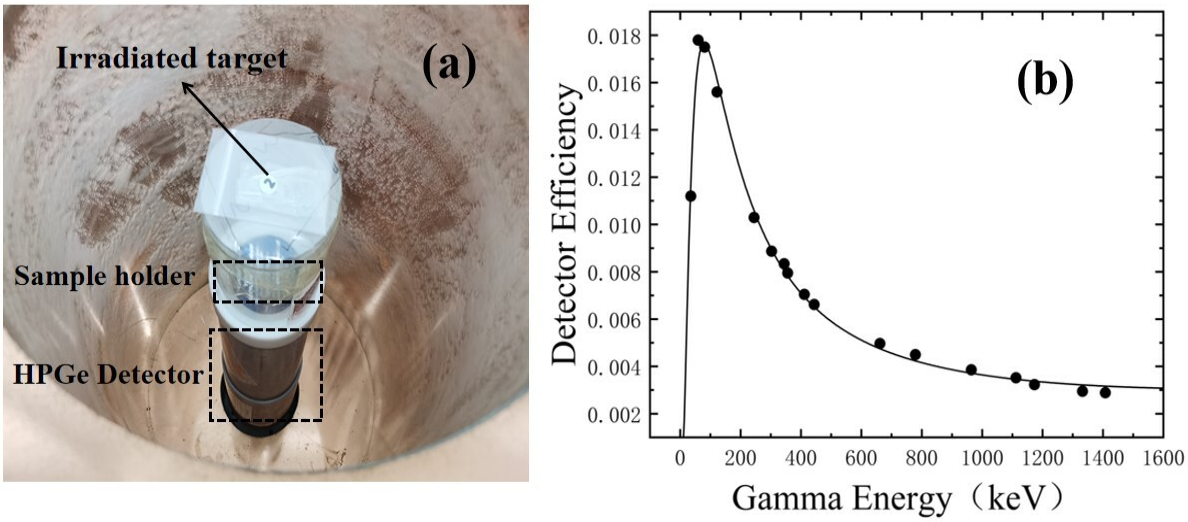

Fig. 4. ORTEC GMX 50P4-83 HPGe detector (a) and corresponding efficiency at a distance of 10 cm (b).

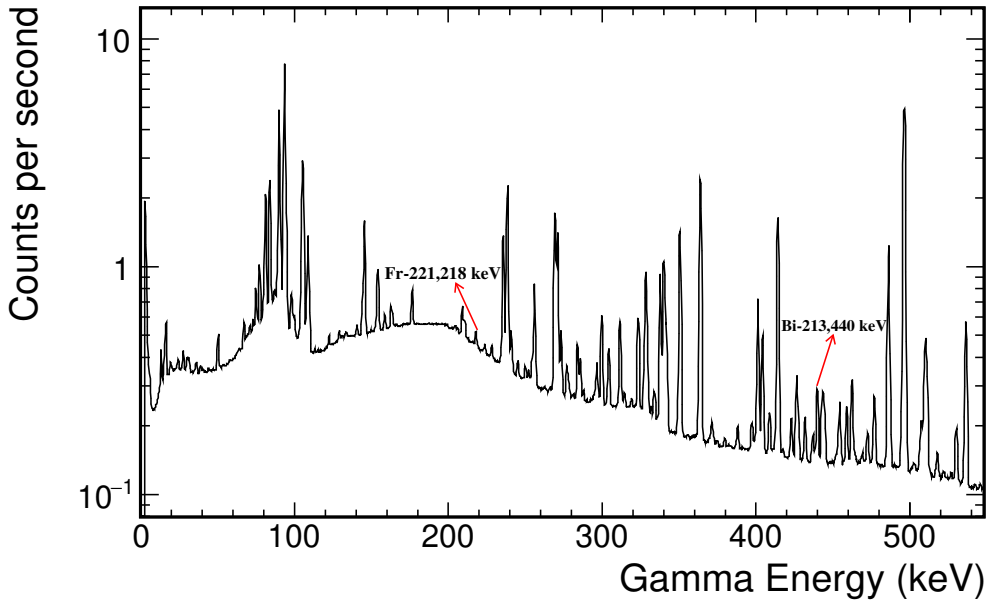

Fig. 5. Gamma-ray spectra of the Th target within 5.03 h of irradiation by 80 MeV protons and after 27.76 days of cooling after the EOB. Characteristic gamma peaks of ^{221}Fr and ^{213}Bi are visible in the figure.

and nuclear scattering with graphite when the beam flies through the degrader, which is the major contributor to the proton-energy spread. Generally, as the thickness of the degrader increases, the spread of the proton energy widens. The proton-energy resolution was obtained in our previous studies based on the activation-analysis measurements and FLUKA simulations[13, 21]. Table 3 lists the proton-energy resolutions used in this experiment, which were calculated by di-

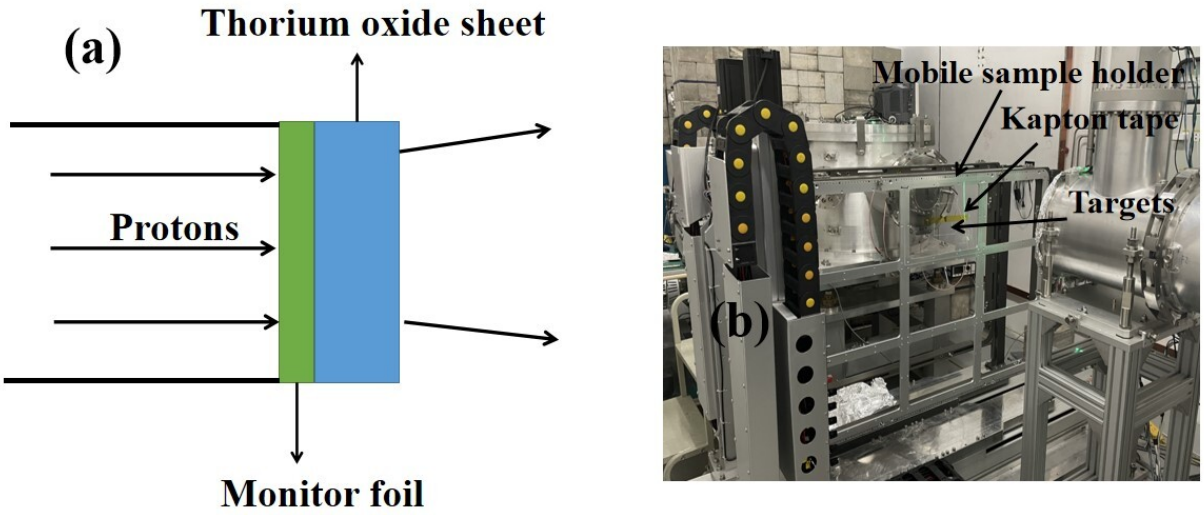

Fig. 6. (a) Irradiation schematic and (b) experimental setup for the thorium oxide sheet and monitor foil at APEP.

viding the full width at half maximum E_{FWHM} by the peak energy E_0. The energy-resolution data in the table were used as the lateral uncertainties of the experimentally measured excitation function.

Table 3. Energy resolution of proton at different energy points.

E_0(MeV)	Energy resolution	$E_{FWHM}/2$(MeV)
80	5.46%	2.19
70	3.63%	1.27
60	3.74%	1.12
50	4.49%	1.13
40	7.49%	1.50

B. Determination of ^{232}Th(p, x)^{225}Ac reaction cross section

The yield of ^{225}Ac is related to the ^{232}Th(p, x)^{225}Ac reaction cross section and proton flux via the well-known formula[24]

$$A_0 = N\sigma_{px}\phi(1 - e^{-\lambda t_i}), \tag{1}$$

where A_0 is the EOB radioactivity of ^{225}Ac (dps), N is the areal density of the target (atom/cm^2), ϕ is the average proton flux (protons/s), σ_{px} is the reaction cross-section for the formation of ^{225}Ac (cm^2), λ is the decay constant of the radioisotope of interest (s^{-1}), and t_i is the irradiation time (s). A_0 can be determined through the activation method using the characteristic gamma peak measured by the HPGe, which can be expressed as

$$A_0 = \lambda C(\frac{t_m}{t_l})/(\varepsilon_p I_\gamma e^{-\lambda t_c}(1 - e^{-\lambda t_m})), \tag{2}$$

where C is the full-energy peak area of the measured characteristic gamma ray. I_γ is the branching intensity of the characteristic gamma ray and ε_p is the corresponding detection efficiency. t_c, t_m, and t_l represent the cooling, real-measurement, and live times, respectively. The term $\frac{t_m}{t_l}$ represents the dead-time correction. With Eq. (1) and Eq. (2), the reaction cross section can be determined as follows:

$$\sigma_{px} = \frac{\lambda C(\frac{t_m}{t_l})}{N\phi\varepsilon_p I_\gamma(1 - e^{-\lambda t_m})e^{-\lambda t_c}(1 - e^{-\lambda t_i})}. \tag{3}$$

To determine an accurate cross section, the proton flux (ϕ) incident on the target must be measured. In this study, the absolute value of the proton flux was determined by placing monitor foils in front of the target. Based on the standard reaction cross section of protons and monitor-foil nuclei, the incident proton flux ϕ can be deduced from the following equation:

$$\sigma_m = \frac{\lambda_m C_m(\frac{t_{mm}}{t_{lm}})}{N_m\phi\varepsilon_m I_m(1 - e^{-\lambda_m t_{mm}})e^{-\lambda_m t_{cm}}(1 - e^{-\lambda_m t_{im}})}, \tag{4}$$

where the subscript "m" represents the Cu monitor foil. t_{cm}, t_{mm}, and t_{lm} are the cooling time, real-measurement time, and live time of the irradiated copper, respectively. The values of the standard cross sections σ_m were sourced from the

standard charged-particle cross-section database of the International Atomic Energy Agency (IAEA)[25]. The ^{nat}Cu (p, x) ^{58}Co reaction was selected to monitor the proton beam because of the specific shape of the excitation function, with the cross section showing two resonance peaks at approximately 40 and 100 MeV[26]. The long-lived product ^{58}Co ($T_{1/2}$=70.86 d, 99.45% γ) decays with a strong characteristic γ-ray of 810 keV, which allows for prolonged activity measurements days after the EOB. In the experiment, the monitor foil and Th sheet were bound together, irradiated with protons simultaneously under the same conditions, and then measured separately using the HPGe detector. The proton flux through the thin monitor foil and the target is considered to be consistent; thus, the cross section σ_{px} can be calculated as follows:

$$\sigma_{px} = \frac{\lambda C(\frac{t_m}{t_l})}{\lambda_m C_m(\frac{t_{mm}}{t_{lm}})} \times \frac{N_m \varepsilon_m I_m}{N \varepsilon_p I_\gamma} \times \frac{(1-e^{-\lambda_m t_{mm}})e^{-\lambda_m t_{cm}}(1-e^{-\lambda_m t_{im}})}{(1-e^{-\lambda t_m})e^{-\lambda t_c}(1-e^{-\lambda t_i})} \times \sigma_m. \quad (5)$$

The variables in Eq. (5) have the same meaning as in Eq. (3) and Eq. (4). After irradiation, an adequate measurement time for the monitor foils was ensured to maintain statistical uncertainties below 1%.

C. Correction of ^{232}Th(p, x)^{225}Ac reaction cross section

In actual measurements, many factors inevitably impact the final value of the cross section, and several components contribute to the uncertainty of the measured data. For the experimental data, the necessary corrections must be made with the help of theoretical simulations and calculations. Because of the thick samples used in this study, the corrections to be considered include the following components: (1) self-absorption of gamma rays, (2) attenuation of proton flux and energy, and (3) scattering effects of protons. Other factors, such as the mass and geometric parameters of the samples, are more inconsequential and can be ignored.

Gamma rays interact with a sample through the photoelectric effect, electron-positron pair effect, and Compton scattering when emitted from a sample with a finite thickness, resulting in gamma attenuation. This self-absorption effect causes fewer gamma rays to be detected by the HPGe detector than those emitted from the activated sample, thereby affecting the measurement results of the cross section (Eq. (5)). Because the contribution of this effect is difficult to deduce through experiments, the correction factor of self-absorption was estimated using the following formula:

$$f_g = \frac{\mu_m x}{1-e^{-\mu_m x}}, \quad (6)$$

where $\mu_m = \mu/\rho$ is the mass-attenuation coefficient, which was acquired from the NIST Standard Reference Database 126[27]. The mass thickness x is defined as the mass per unit area, which is obtained by multiplying the sample thickness t by the density ρ, that is $x = \rho t$. f_g represents the integrated effect of the gamma attenuation at different thicknesses within the sample.

During irradiation, self-shielding occurs when protons pass through a sample with a certain thickness. Self-shielding is a reduction in the observed cross-section due to interactions between incident protons and other nuclei in front of the current position. In this scenario, as protons progressively undergo nuclear reactions with the sample, this results in flux attenuation, causing the parameter ϕ in Eq.(1) to be smaller than the measured value. Additionally, proton-energy attenuation occurs because of reactions between protons and the target nuclei, which leads to a shift in the yield. To estimate the correction factor (f_a) of the proton flux and energy attenuation, the yield of ^{225}Ac produced at different sample depths was calculated using the Geant4 Monte Carlo code because of its flexible features of particle tracking[28]. The QGSP_INCLXX_HP physics list and G4TENDL database were adopted. In the simulation, the sample target was divided into n layers to ensure that each layer had a thickness of approximately 20 μm, with each layer corresponding to the number of ^{225}Ac nuclei as Y_1, Y_2 ,...,Y_i,...,Y_n [29]. The attenuation-correction factor was calculated as follows:

$$f_a = \frac{nY_1}{\sum_{i=1}^{i=n} Y_i}, \quad (7)$$

where Y_i represents the amount of ^{225}Ac produced in the ith layer.

Another aspect requiring correction is the increase in the yield of radioactive isotopes resulting from proton scattering. In the experiment, protons scattered from the Kapton tape, beam monitor foil, and sample cladding material interacted with the irradiated sample, resulting in a non-negligible interference with the production of radioactive isotopes in the activated sample. Furthermore, some of the protons scattered from the irradiated sample increase the isotope yield in the monitor foil, thereby affecting the measurement results. Therefore, the scattering effect f_s of protons must be corrected. This factor was calculated using a simulation. The irradiation model was constructed using the FLUKA code. First, we calculated the yield of radioactive nuclides B_R produced in the sample under real experimental conditions. Under ideal conditions, we obtained the yield of radioactive nuclides B_I in the sample when no protons were scattered. The scattering-effect factor of the sample (f_{ss}) was then calculated as

$$f_{ss} = \frac{B_I}{B_R}. \quad (8)$$

The same correction was applied to the monitor foils and the scattering-effect factor of the monitor foils (f_{sm}) was calculated using the same method as in Eq. (8). The final scattering-effect factor f_s was deduced using the formula $f_s = f_{ss}/f_{sm}$. All of the aforementioned correction factors are listed in Table 4. The overall correction factor f was calculated using $f = f_g f_a f_s$. As shown in the table, f_a and f_s are energy-dependent factors, because the attenuation and scattering of protons within the sample are related to the proton energy. In the low-energy range of 40–50 MeV, the ThO_2

sample had an obvious attenuation effect on the proton energy, which led to a noticeable increase in f_a. f_g was independent of the incident proton energy but was related to the target thickness. The marginal differences in the target thicknesses used in different irradiation experiments resulted in variations in f_g at different energies.

Table 4. Correction factors corresponding to different experimental conditions.

Proton energy	Correction factors			
(MeV)	f_g	f_a	f_s	f
80	1.24	1.07	1.02	1.35
70	1.22	0.88	1.06	1.14
60	1.24	0.93	1.06	1.22
50	1.25	1.65	1.06	2.19
40	1.22	1.88	1.10	2.52

The uncertainty in this study consists of several components, including statistical and systematic uncertainties. The statistical uncertainty was estimated using the formula $N^{-0.5}$ for N counts in a full-energy peak. The HPGe detector provided an adequate measurement time to ensure statistical uncertainties of less than 1%. Specifically, near 40 MeV, the statistical uncertainty was between 1% and 2% because of the small cross section. The systematic uncertainties mainly originate from the detector-efficiency calibration (4.8%), area of the gamma peak (0.4%-4.7%), decay data of the reaction products (0.8%), standard cross section of the monitor foils (4.7%–5.4%), and target thickness (0.1%–3.2%). The overall uncertainties (6.8%–9.2%) in the measured cross-section were calculated by summing all individual uncertainties in the quadrature, which are shown in Fig. 7 in the form of error bars for the measured cross-sections.

IV. RESULTS AND DISCUSSION

A. ^{232}Th(p, x)^{225}Ac reaction cross section

The measured cross-sections of the ^{232}Th(p, x)^{225}Ac reaction at proton energies of 80 $\pm$ 2.19 MeV, 70 $\pm$ 1.27 MeV, 60 $\pm$ 1.12 MeV, 50 $\pm$ 1.13 MeV, and 40 $\pm$ 1.50 MeV are show in Fig. 7, accompanied by experimental data from previous measurements and theoretical data from the latest TALYS-based evaluated nuclear-data library (TENDL)-2021[30]. The values are listed in Table 5. The theoretical cross-sectional data in the TENDL were obtained from calculations performed using the computer code TALYS, an open-source software package for the prediction and analysis of nuclear reactions[31]. Theoretical data on proton-nucleus reactions are generally included in this database. The existing experimental data were derived from the Experimental Nuclear Reaction Data (EXFOR)[32]. Based on existing data, the production cross section of ^{225}Ac was small when the proton energy was less than 40 MeV; thus, obtaining valid results through experimental measurements was difficult. The solid curve of the IAEA recommended excitation function in Fig. 7 was evaluated by the Coordinated Research Project of the IAEA (IAEA CRP)[33], and the recommended values of the cross section was downloaded from the Medical Portal of the Nuclear Data Section (IAEA-NDS) website[25]. During the evaluation, the evaluators assigned greater weights to the dataset measured by Weidner et al. (2012)[10] compared to those from other experiments because this dataset covered the widest energy range. Details of the nuclear data-evaluation process can be found in [33].

As presented in Fig. 7, within a reasonable uncertainty, the data from this study are in good agreement with the existing data from the previous measurements for the proton-energy range of 40–80 MeV. Near 80 MeV, the value obtained in this study is marginally higher than that measured by Griswold et al.(2016)[8] and slightly lower than that measured by Weidner et al.(2012)[10]. At 70 and 60 MeV, the present data are consistent with the experimental data from Steyn et al.(2021)[7]. At 50 MeV, our measured data were lower than the existing data. We speculate that around this energy, the cross section varied considerably with the proton energy, and the thick Th target used for the measurements caused pronounced attenuation of the proton energy. This resulted in an energy shift of the protons, leading to a smaller observed cross section. Therefore, thinner targets will be used in future studies to test this hypothesis. For a proton energy of approximately 40 MeV, our data are closer to the data from the IAEA recommendations and the data sets measured by Ermolave et al.(2012)[11], but higher than the measurements by Steyn et al.(2021)[7]. Significant discrepancies exist between the different experimental data in this region, which may be because the proton energy was near the reaction threshold of ^{232}Th(p, x)^{225}Ac.

Overall, the variation trend in the measured excitation function aligned with those depicted in TENDL and by Steyn et al.(2021)[7]. The excitation function exhibited a resonance peak at 50–60 MeV and decreased with increasing energy from approximately 60 MeV to 80 MeV. One possible explanation for the resonance peak near 60 MeV is that the contribution from the ^{232}Th(p, p7n)^{225}Th$\rightarrow$ ^{225}Ac reaction decreased with increasing energy, whereas the contribution from the ^{232}Th(p, 2p6n)^{225}Ac reaction increased in this range (Fig.1). The underlying reason for the peak and its position is the combined effect of particle pre-equilibrium emission and neutron de-excitation, which require further study of the microscopic theoretical mechanisms. An inflection point occurred at approximately 80 MeV, beyond which, the cross section increased progressively with increasing energy. As the proton energy increased, the contribution of the spallation reactions directly producing ^{225}Ac increased, leading to an increase in the reaction cross section from approximately 80 MeV to 200 MeV. Above 200 MeV, more measurements are required to verify the trend in the cross-sectional variation owing to the lack of experimental data. Compared with the evaluated data in TENDL, our measured values were significantly lower, and all existing experimental data show the same phenomenon. The theoretical models used by TALYS overestimated our measurements by factors of 2–12, illustrating the necessity for further elaboration of nuclear models and the requirement for more experimental cross-sectional mea-

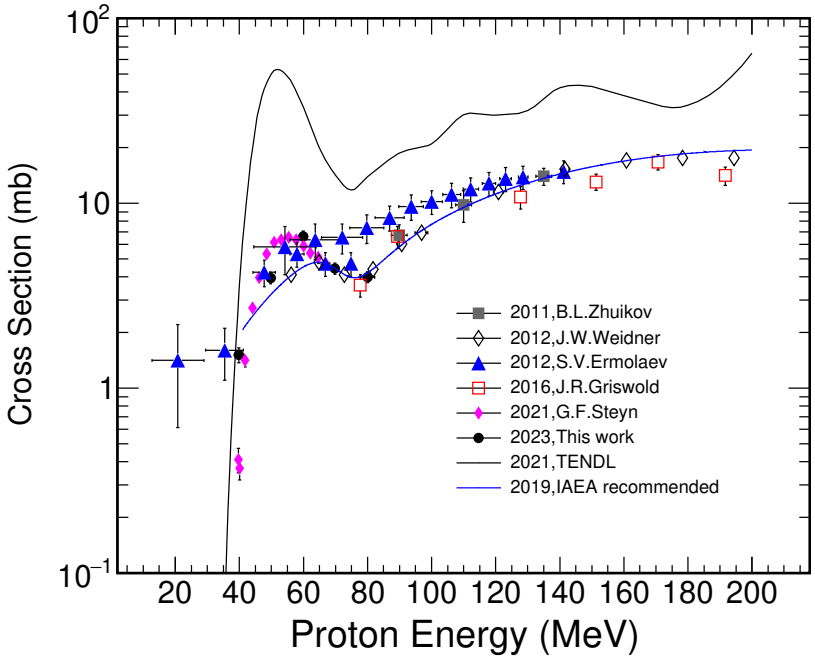

Fig. 7. Comparison of the present experimental data, several existing data from EXFOR, and the evaluated data from TENDL-2021. To keep the figure readable, the uncertainties for part of the existing experimental data are omitted.

Table 5. Measured cross-sections of ^{232}Th(p, x)^{225}Ac in the present and previous works, as well as the recommended theoretical data from TENDL and IAEA.

Proton energy (MeV)	Effective cross section of ^{232}Th(p, x)^{225}Ac						
	This work (mb)	TENDL (mb)	IAEA (mb)	Weidner et al.(2012)[10]	Griswold et al.(2016)[8]	Steyn et al.(2021)[7]	Ermolave et al.(2012)[11]
80 ± 2.19	3.96 ± 0.27	13.97	4.20	4.40 mb (81.77 MeV)	3.60 mb (77.80 MeV)	–	7.30 mb (79.90 MeV)
70 ± 1.27	4.43 ± 0.31	14.16	4.43	4.10 mb (72.87 MeV)	–	4.73 mb (66.97 MeV)	6.50 mb (72.20 MeV)
60 ± 1.12	6.59 ± 0.47	32.88	4.53	–	–	5.89 mb (60.00 MeV)	5.30 mb (58.00 MeV)
50 ± 1.13	3.92 ± 0.29	50.12	3.23	–	–	6.16 mb (50.80 MeV)	4.20 mb (47.90 MeV)
40 ± 1.50	1.51 ± 0.14	3.53	2.10	–	–	0.365 mb (40.25 MeV)	1.60 mb (35.60 MeV)

surements to accurately determine isotope-production yields and enhance these models.

B. In-target production yields

Based on the cross sections measured in the present work, the yields of ^{225}Ac produced by irradiating a Th target with protons at different energies can be assessed. Considering the proton flux and reaction cross section, preliminary experiments for ^{225}Ac production will be conducted at APEP using 80 MeV protons. Based on the previous results of beam-flux measurements at APEP, we observed that a 10-MeV decrease in proton energy results in a flux reduction of several times, owing to the blocking effect of the energy degrader[21]. Below 80 MeV, the flux loss caused by the energy degrader reduces the production yield of ^{225}Ac, outweighing the benefits gained from the increased cross section. Therefore, protons with an energy of 80 MeV were used to produce ^{225}Ac to maximize the yield at CSNS APEP.

The EOB yields for ^{225}Ac assuming a continuous 6-day irradiation of Th targets of a specific thickness by 80-MeV protons with different proton currents are outlined in Table 6. For comparison, the yields calculated from the IAEA website[34] are also listed in this table. The table shows that irradiating a thick Th target with 80-MeV protons at APEP can easily achieve an EOB yield of ^{225}Ac at the millicurie level. Assuming a conservative chemical-separation efficiency of approximately 6%, irradiating a 2-g/cm^2 target of ^{232}Th with 1 kW and 80-MeV protons for one day (24 h) can yield hundreds of microcuries of ^{225}Ac after separation, which is sufficient for conducting clinical trials. With increased accelerator power at CSNS, irradiating a Th target with a thickness of 5 g/cm^2 using 5 kW and 80-MeV protons continuously for 6 days can yield up to 10 mCi of ^{225}Ac after separation. Owing to the 5000 h/year operating time of CSNS, the annual production

Table 6. Production yields of ^{225}Ac calculated by the measured cross section and IAEA database. The value of the measured cross section is derived from Table 5.

Energy (MeV)	Power (kW)	Current (μA)	Irradiation Time (day)	Mass thickness (g/cm^2)	EOB yield (mCi)	
					This work	IAEA calculation
80	1	12.5	1	2	2.93 $\pm$ 0.20	2.99
80	5	62.5	6	5	185.72 $\pm$ 12.66	204.63

of ^{225}Ac is approximately 340 mCi, which is substantial compared to the current annual worldwide supply ($\sim$ 2 Ci). The irradiation schemes listed in Table 6 will be used as routine modes for CSNS APEP in the future.

As shown in the table, the EOB yields were theoretically calculated using the experimental cross sections measured in this study based on the idealization of the radioisotope-production process. In practice, several factors reduce the final yield of ^{225}Ac, including target thickness, target impurities, beam current, and chemical-separation methods. Achieving a high yield of ^{225}Ac also depends on high-performance targets and stable proton beams. This summer, preliminary research experiments focused on ^{225}Ac production and the associated chemical-separation processes will be conducted at CSNS APEP, and we will provide ongoing updates on our progress.

V. CONCLUSION

The cross sections of the ^{232}Th(p, x)^{225}Ac reaction at proton energies of 80 $\pm$ 2.19 MeV, 70 $\pm$ 1.27 MeV, 60 $\pm$ 1.12 MeV, 50 $\pm$ 1.13 MeV, and 40 $\pm$ 1.50 MeV have been experimentally determined using the activation method and off-line gamma-ray spectrometric technique, which provides a significant addition to the published ^{225}Ac data up to 80 MeV. The experimental data were in good agreement with existing data measured at other facilities. Additionally, the variation trend in the measured excitation functions was in good agreement with that depicted in TENDL. The results showed that the experimental cross sections of the ^{232}Th(p, x)^{225}Ac reaction are lower than those shown in the theoretical data. The measured cross sections enriched the experimental database and improved the quality of the evaluated nuclear-data libraries and theoretical models. Additionally, the results indicated that further measurements of the ^{232}Th(p, x)^{225}Ac reaction cross sections are required to enhance the reliability of the theoretical data.

This work is the first experiment to measure proton-nuclear reaction cross sections conducted at CSNS. Our study illustrates that the APEP is equipped to perform measurements of cross sections for the formation of medical isotopes, satisfying both the prerequisites for proton irradiation and the requirements for the HPGe detector. The data presented in this work will aid in the scaled production of ^{225}Ac through the proton irradiation of ^{232}Th, which offers important guidance for the subsequent chemical purification of ^{225}Ac for medical applications. As documented, multi-millicurie quantities of ^{225}Ac can be produced in a single 6-day irradiation of a 5 g/cm^2 Th target at CSNS APEP when it reaches a beam power of 5 kW. In the immediate future, chemical-separation experiments for the production of ^{225}Ac will be conducted at CSNS, and we will report the development of related designs of the target station and the results of the chemical processing.

VI. ACKNOWLEDGMENTS

This study was supported by the National Natural Science Foundation of China (Grant Numbers 12075135 and 12375127).

VII. BIBLIOGRAPHY

[1] Y. S. Kim, M. W. Brechbiel, An overview of targeted alpha therapy. Tumor Biol. **33**, 573-590 (2012). doi: 10.1007/s13277-011-0286-y

[2] A. Morgenstern, C. Apostolidis, C. Kratochwil *et al.*, An overview of targeted alpha therapy with ^{225}Actinium and ^{213}Bismuth. Curr. Radiopharm. **11**, 200-208 (2018). DOI: 10.2174/1874471011666180502104524

[3] A.A.A.Qaaod, V.Gulik, ^{226}Ra irradiation to produce ^{225}Ac and ^{213}Bi in an accelerator-driven system reactor. Nucl. Sci. Tech. **31**, 44 (2020). doi: 10.1007/s41365-020-00753-2

[4] S. Hogle, R.A. Boll, K. Murphy *et al.*, Reactor production of Thorium-229. Appl. Radiat. Isot. **114**, 19-27 (2016). DOI: 10.1016/j.apradiso.2016.05.002

[5] A. K. H. Robertson, C. F. Ramogida, P. Schaffer *et al.*, Development of ^{225}Ac radiopharmaceuticals: TRIUMF perspectives and experiences. Curr. Radiopharm. **11**, 156-172(2018). DOI: 10.2174/1874471011666180416161908

[6] B. L. Zhuikov, S. N. Kalmykov, S.V. Ermolaev *et al.*, Production of ^{225}Ac and ^{223}Ra by irradiation of Th with accelerated protons. Radiochemistry. **53**, 73-80 (2011). DOI: 10.2174/1874471011666180416161908

[7] G. F. Steyn , M. A. Motetshwane, F. Szelecsényi *et al.*, Pairing of thorium with selected primary target materials in tandem configurations: Co-production of ^{225}Ac/^{213}Bi and ^{230}U/^{226}Th generators with a 70 MeV H cyclotron. Appl. Radiat. Isot. **168**, 109514 (2021). DOI: 10.1016/j.apradiso.2020.109514

[8] J. R. Griswold , D. G. Medvedev, J. W. Engle *et al.*, Large scale accelerator production of ^{225}Ac: Effective cross sections for 78-192 MeV protons incident on ^{232}Th targets. Appl. Radiat. Isot. **118**, 366-374 (2016). DOI: 10.1016/j.apradiso.2016.09.026

[9] J. W. Weidner , S. G. Mashnik, K. D. John *et al.*, ^{225}Ac and ^{223}Ra production via 800 MeV proton irradiation of natural thorium targets. Appl. Radiat. Isot. **70(11)**, 2590-2595 (2012). DOI: 10.1016/j.apradiso.2012.07.003

[10] J. W. Weidner , S. G. Mashnik, K. D. John *et al.*, Proton-induced cross sections relevant to production of ^{225}Ac and ^{223}Ra in natural thorium targets below 200 MeV. Appl. Radiat. Isot. **70(11)**: 2602-2607 (2012). DOI: 10.1016/j.apradiso.2012.07.006

[11] S. V. Ermolaev, B. L. Zhuikov, V. M. Kokhanyuk *et al.*, Production of actinium, thorium and radium isotopes from natural thorium irradiated with protons up to 141 MeV. Radiochimica Acta. **100(4)**, 223-229 (2012). DOI: 10.1524/ract.2012.1909

[12] L.Wang , Y. Lyu , F. Wang *et al.*, Experimental Study on Production of Medical Nuclide ^{225}Ac with 100 MeV Cyclotron (in Chinese). At. Energy Sci. Technol. **55 (zengkan)**: 171(2021). DOI: 10.7538/yzk.2020.youxian.0798

[13] Y.Liu , H.Jing , L.Huang *et al.*, Physical design of the APEP beam line at CSNS. Nucl. Instrum. Methods Phys. Res. A **1042**, 167431(2022). DOI: 10.1016/j.nima.2022.167431

[14] J. Wei , H. Chen , Y. Chen *et al.*, China spallation neutron source: design, R&D, and outlook. Nucl. Instrum. Methods Phys. Res. A **600(1)**, 10-13(2009). DOI: 10.1016/j.nima.2008.11.017

[15] J. Wei, S. N. Fu, G. Y. Tang *et al.*, China Spallation Neutron Source-an overview of application prospects. Chin. Phys. C **33(11)**, 1033(2009). DOI: 10.1088/1674-1137/33/11/021

[16] H.Chen , X. L. Wang, China's first pulsed neutron source. Nat. Mater. **15(7)**, 689-691 (2016). DOI: 10.1038/nmat4655

[17] B. Jiang, B. B. Tian, H. T. Jing *et al.*, Feasibility of medical radioisotope production based on the proton beams at China Spallation Neutron Source. Nucl. Sci. Tech. **35**, 102 (2024). DOI: 10.1007/s41365-024-01438-w

[18] S.Wang ,Y.W. An ,S. X. Fang *et al.*, An overview of design for CSNS/RCS and beam transport. Sci. China: Phys. Mech. Astron. **54**, 239-244 (2011). DOI: 10.1007/s11433-011-4564-x

[19] F. Wang, T. Liang, W. Yin *et al.*, Physical design of target station and neutron instruments for China Spallation Neutron Source. Sci. China: Phys. Mech. Astron. **56**, 2410–2424 (2013). DOI: 10.1007/s11433-013-5345-5

[20] J.Y. Tang, Q. An, J.B. Bai *et al.*, Back-n white neutron source at CSNS and its applications. Nucl. Sci. Tech. **32**, 11 (2021). DOI: 10.1007/s41365-021-00846-6

[21] W. Li , Q. Dong , H.Jing *et al.*, Measurements of proton beam flux and energy of APEP using foil activation technique. Nucl. Eng. Technol. **56**, 328-334 (2023). DOI: 10.1016/j.net.2023.10.004

[22] National Nuclear Data Center (NNDC). https://www.nndc.bnl.gov/

[23] G. Battistoni, F. Cerutti, A. Fasso *et al.*, The FLUKA code: Description and benchmarking. AIP Conf. Proc. Am. Inst. Phys. **896(1)**, 31-49 (2007). DOI: 10.1063/1.2720455

[24] R. Michel , R. Bodemann, H. Busemann *et al.*, Cross sections for the production of residual nuclides by low-and medium-energy protons from the target elements C, N, O, Mg, Al, Si, Ca, Ti, V, Mn, Fe, Co, Ni, Cu, Sr, Y, Zr, Nb, Ba and Au. Nucl. Instrum. Methods Phys. Res. B **129(2)**, 153-193 (1997). DOI: 10.1016/S0168-583X(97)00213-9

[25] IAEA Nuclear Data Service. https://www-nds.iaea.org/medical/

[26] A. Hermanne, A. V. Ignatyuk, R. Capote *et al.*, Reference cross sections for charged-particle monitor reactions. Nucl. Data Sheets **148**, 338-382(2018). DOI: 10.1016/j.nds.2018.02.009

[27] NIST Standard Reference Database 126. https://www.nist.gov/pml/x-ray-mass-attenuation-coefficients

[28] Agostinelli S, Allison J, Amako K *et al.*, GEANT4—a simulation toolkit. Nucl. Instrum. Methods Phys. Res. A **506(3)**, 250-303(2003).DOI: 10.1016/S0168-9002(03)01368-8

[29] S. Shen, Z. Yuan, X. Luo *et al.*, Measurement of ^{232} Th neutron capture cross-sections in the energy range of 2.0-5.0 MeV by using the neutron activation technique. Nucl. Instrum. Methods Phys. Res. B **476**, 59-63 (2020). DOI: 10.1016/j.nimb.2020.04.028

[30] TALYS based evaluated nuclear data library. https://tendl.web.psi.ch/tendl_2021/tendl2021.html

[31] A. J. Koning, D. Rochman, Modern nuclear data evaluation with the TALYS code system. Nucl. Data Sheets **113(12)**, 2841-2934 (2012). DOI: 10.1016/j.nds.2012.11.002

[32] Experimental Nuclear Reaction Data (EXFOR). https://www-nds.iaea.org/exfor/

[33] J. W. Engle , A. V. Ignatyuk , R. Capote *et al.*, Recommended nuclear data for the production of selected therapeutic radionuclides. Nucl. Data Sheets **155**, 56-74 (2019). 10.1016/j.nds.2019.01.003

[34] Medical Isotope Browser. https://www-nds.iaea.org/relnsd/isotopia/isotopia.html